Supporting Material

For: Exchangeable colloidal AFM probes for the quantification of irreversible and long term interactions

Pablo Dörig, Dario Ossola, Anh Minh Truong, Monika Graf, Flurin Stauffer, János Vörös, Tomaso Zambelli

Laboratory of Biosensors and Bioelectronics, Institute of Biomedical Engineering, ETH Zurich, Gloriastrasse 35, 8092 Zurich, Switzerland

Measurement of flow through a FluidFM cantilever

The flow through a tipless FluidFM cantilever was measured by tracking single fluorescent colloids (175nm, P7220, Invitrogen) in HEPES2 buffer on an inverted microscope. The pressure was varied from 0 to 20 mbar as shown in Fig. S1.

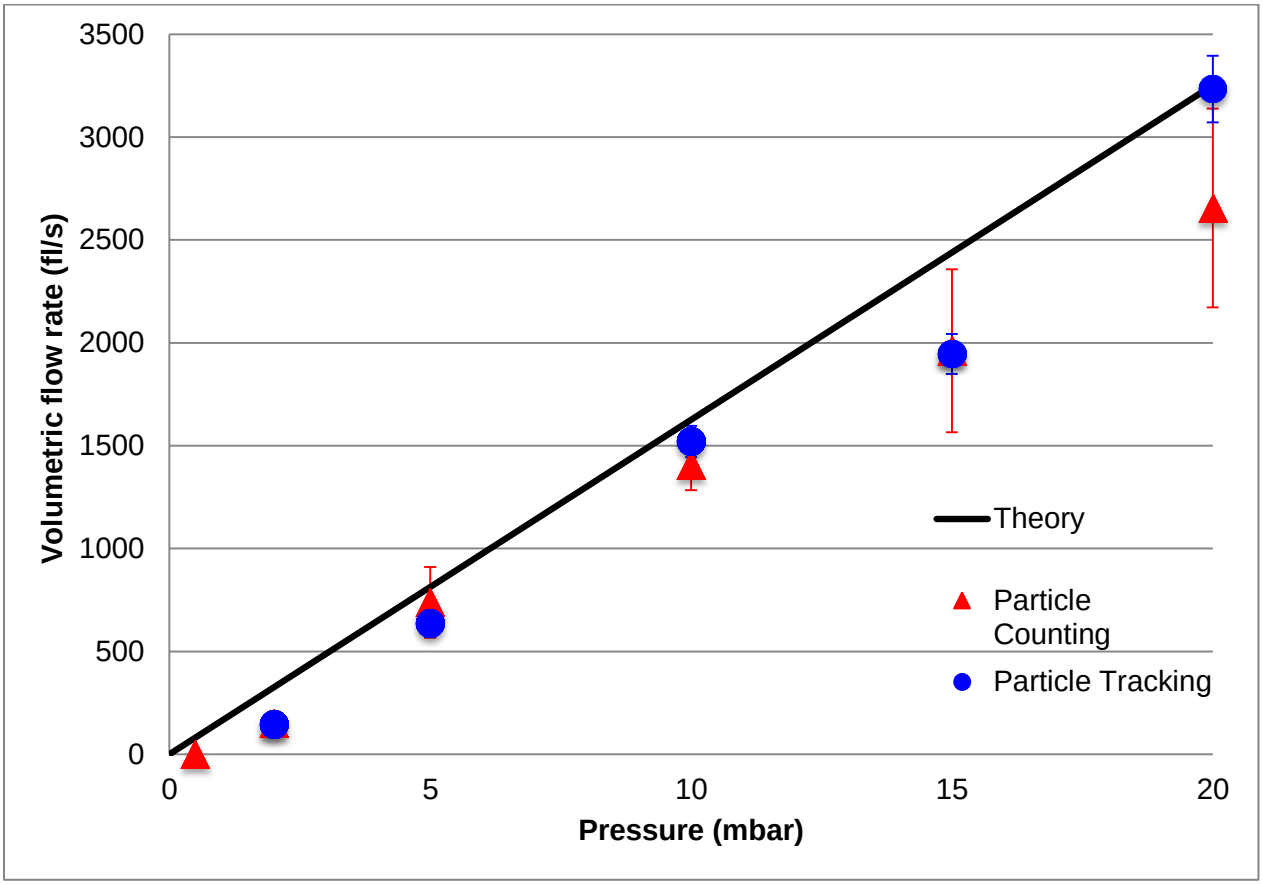

Figure S1: Measured vs. theoretical flow in a tipless FluidFM cantilever

Two independent methods were used to validate the results:

A) For the **particle counting** we monitored how many particle crossed a certain line in the cantilever in a given time, combined with the known particle density in solution this translated into a volumetric flow (n=1000 particles).
B) **Particle tracking** relied on the measured flow profile in the channel (Fig. S2, n=250 particles), the fastest observed particles then allowed to calculate the total volumetric flow.

For the theoretical flow only the hydrodynamic resistance of the cantilever channel and its opening were considered. Calculations showed that the cantilever opening did not affect the overall flow resistance if it was larger than 1 µm in diameter. This was the case for all cantilevers in this study. As sketched in Fig. S2 there are pillars in the channel for structural stabilization. The effect of these pillars on the flow was analyzed with COMSOL and corresponded to an increase of the flow resistance by 7 percent. This increased resistance is already represented in Fig. S1.

Fig. S2 displays the measured flow profile in the FluidFM channel. The two observed minima are due to support pillars in the channel, which are shown schematically on the left side of the figure.

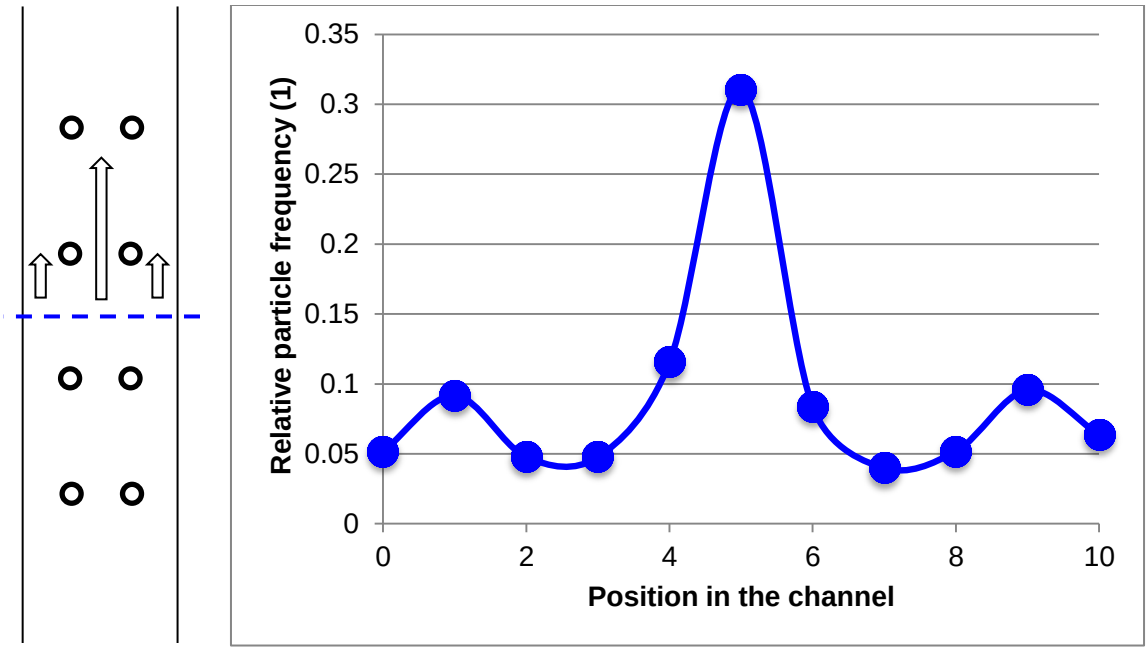

Figure S2: Particle flow distribution in the channel. The channel was divided into 10 equidistant segments and the particle flow was monitored for each segment (n=250 particles). The circles indicate the measured data, while the connecting line is an EXCEL interpolation.

Fluorescence measurement of leak flow

When a polystyrene bead blocks the FluidFM channel opening due to applied suction the quality of the sealing can be assessed by observing the leak flow. Here the channel in the cantilever was filled with a fluorescent solution from a large reservoir in the cantilever holder. The cantilever was immersed in a clear buffer solution, which contained polystyrene beads. The total fluorescence of the 200 µm cantilever was evaluated at different stages. As shown in Fig. S3 and S4 the cantilever is brightest when filled completely with fluorescent solution, a short suction pulse then fills the cantilever with clear buffer and thus drastically reduces its brightness. Then a bead is attracted which blocks the channel opening. Despite the applied suction pressure the cantilever fluorescence recovers, which indicates that the diffusive flow of the fluorophore is larger than the leak flow.

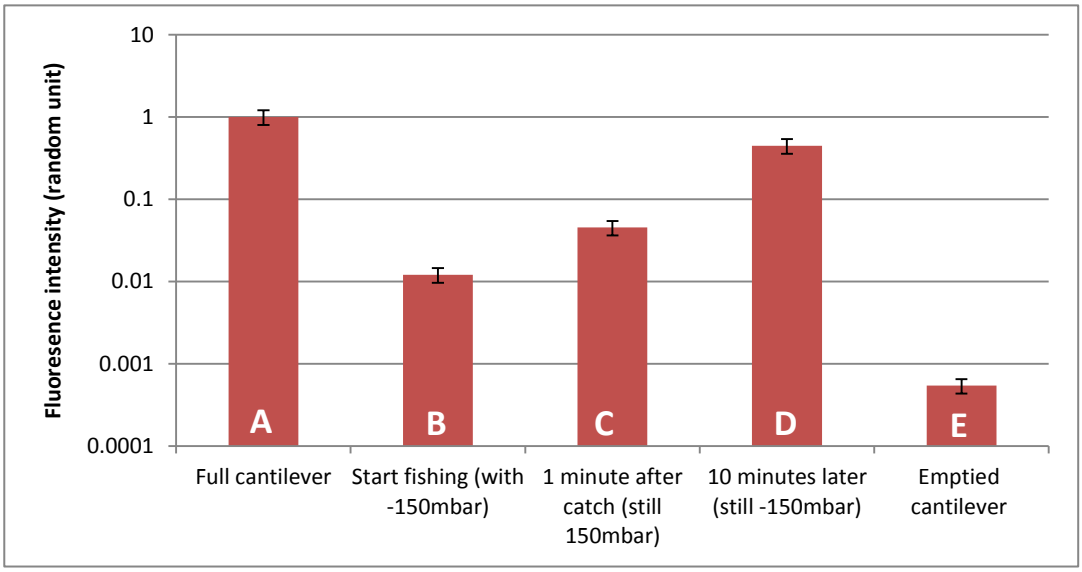

Figure S3: Fluorescence Recovery of cantilever while bead is attached by underpressure

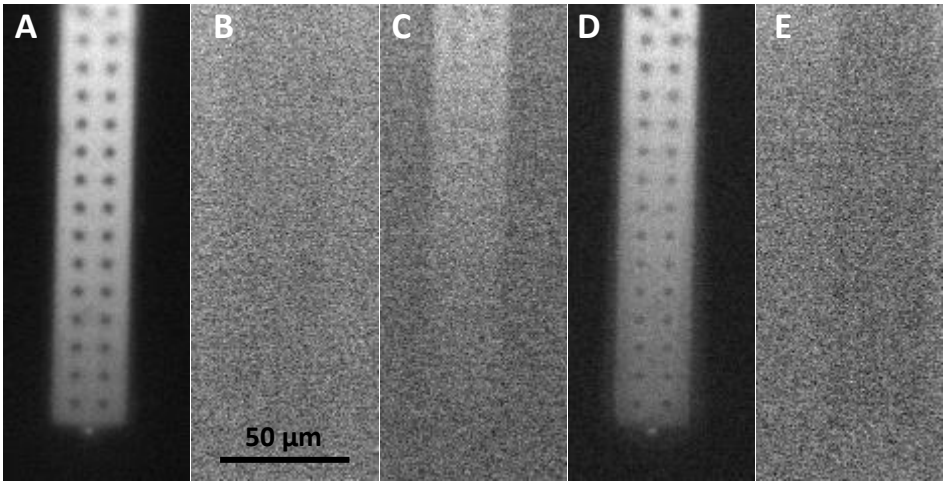

Figure S 4: Fluorescence images of cantilever while bead is attached by underpressure

The fluorescence inside the cantilever was analyzed on the raw images; however for better visibility here they are presented contrast enhanced. The following labels apply for both Fig. S3 and S4:

A) The cantilever is full
B) -150 mbar was applied for a few seconds
C) A bead blocked the exit since 1 minute (-150 mbar)
D) The same bead blocked the exit since 10 minutes (-150 mbar)
E) Thoroughly emptied cantilever

Electric and hydrodynamic resistance with a bead blocking the opening

Introduction

As explained in the main article, the electrical and hydrodynamic resistance of a 3µm spherical bead almost blocking a 2µm circular channel entrance was calculated in COMSOL. The problem was treated as 2D radial symmetric case, where the sphere and the normal of the opening shared the same axis. The sphere and the opening had a small gap *g* between them, which was varied from 0.1nm to 10nm. The buffer solution was assumed to have all the material properties of water at room temperature, except for a higher conductivity of 1.5 S m^{-1}. The 2D geometry of the simulation considers only the liquid part of the system, shown in Fig. S5 and S6 with streamlines. Standard COSMOL interfaces where used for the calculations; *spf* for the fluidics and *ec* for the electrical current.

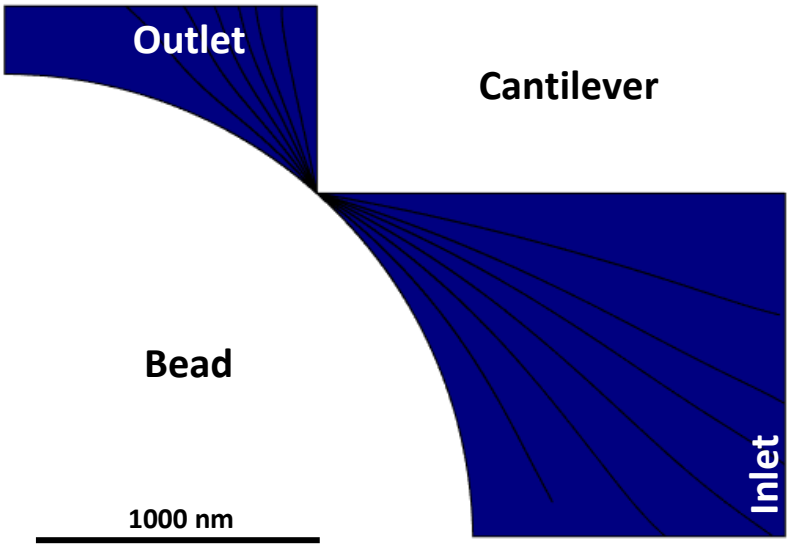

Figure S 5: The 2D COMSOL model. The axis of rotational symmetry is at the left end of the blue buffer. The spherical bead is represented by the circular cavity in the lower left, whereas the cantilever wall shows as rectangle in the upper right. The inlet is along two edges, whereas the outlet is only on the upper most edge.

A strong zoom revealed the gap between bead and cantilever in Fig. S6. Locally around the gap the streamlines were spread radially along the vertical axis. At this close range the geometry could be approximated by two circle sectors. The central angles of these sectors were related to the bead diameter d_b and the opening d_o:

$$\alpha_1 = \cos^{-1}[d_o/d_b]$$
$$\alpha_2 = \sin^{-1}[d_o/d_b]$$

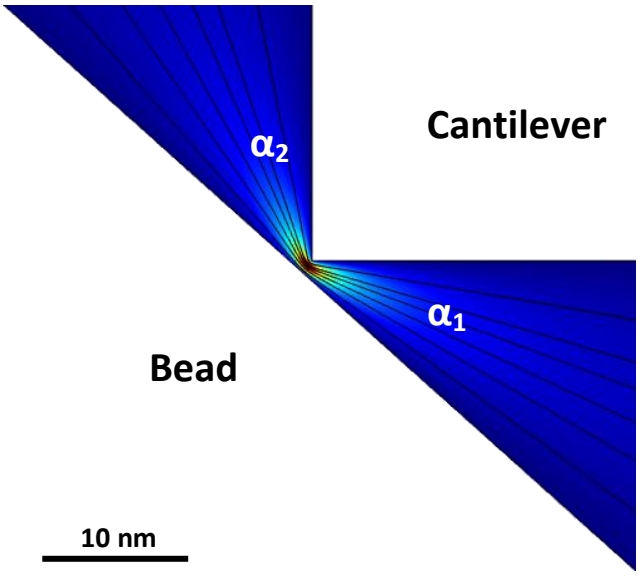

Figure S 6: Zoom in of the COMSOL model with streamlines. The flow velocity is highest (*red*) just at the gap, and then quickly drops to lower values (*blue*) with increasing distance.

Hydrodynamic resistance

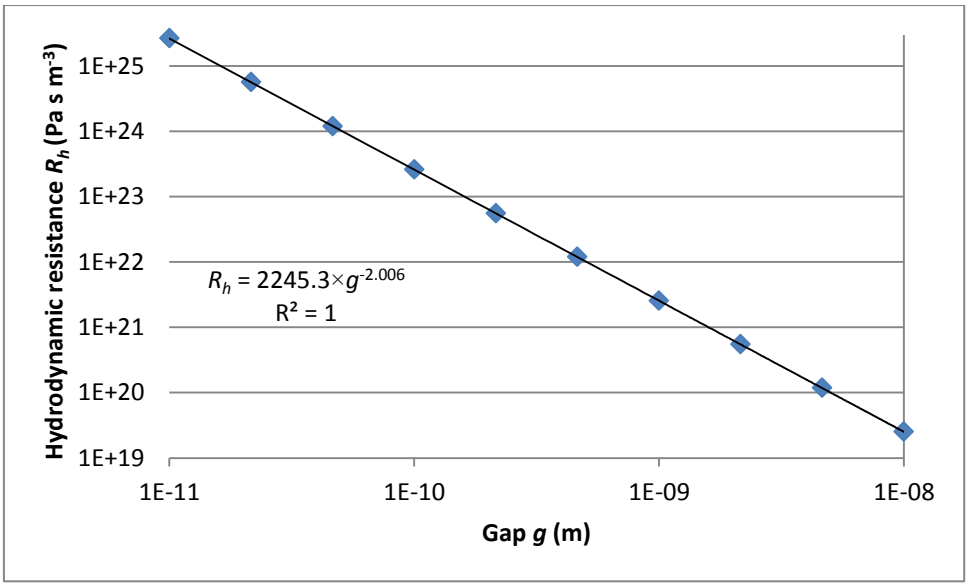

Figure S 7: The simulated hydrodynamic resistance vs. the gap distance and its fitting function. The errors of the simulation are within the rectangle boundaries.

The simulated hydrodynamic resistance scaled with g^{-2} as shown in Fig. S7. An analytic approximation gave the same result. Several assumptions were made to simplify the problem:

- The geometry just around the gap could be considered as two overlapping circle sectors. Each sector originated very close to the gap at a distance x_0.

$$x_0 = \frac{g}{\alpha}$$

  Where α stands for the respective central angle of each sector.

- The sector resistance could be approximated trough an integration of the parallel case along the sector boundaries.
- The annular gap between bead and cantilever could be approximated as a parallel plate segment. The parallel plate resistance is (1):

$$R_{h\ parallel} = 12\frac{\eta l}{wd^3}$$

  Where η is the dynamic viscosity, l the length, d the height and w the width of the parallel plate segment. For this geometry w was:

$$w = \pi d_o$$

- The stream lines are radially spread along the vertical axis, and thus the effective channel height d corresponds to the arc length:

$$d(x) = \alpha \times x$$

  Where x is the distance from the sector origin.

The hydrodynamic resistance R_h of such a sector was mainly determined by the gap g:

$$R_h = 12\eta \int_{x_0}^{\infty} \frac{1}{wd^3} dx = \frac{6\eta}{\pi d_o \alpha} \frac{1}{g^2} \propto g^{-2}$$

Thus, the scaling with g^{-2} could be confirmed. Both sectors combined gave a resistance which only differed by 20% from the exact values found through simulation. Including a finite upper integration limit, considering w a function of x and using the circle geometry instead of a sector did virtually not change the integration result.

Electrical resistance

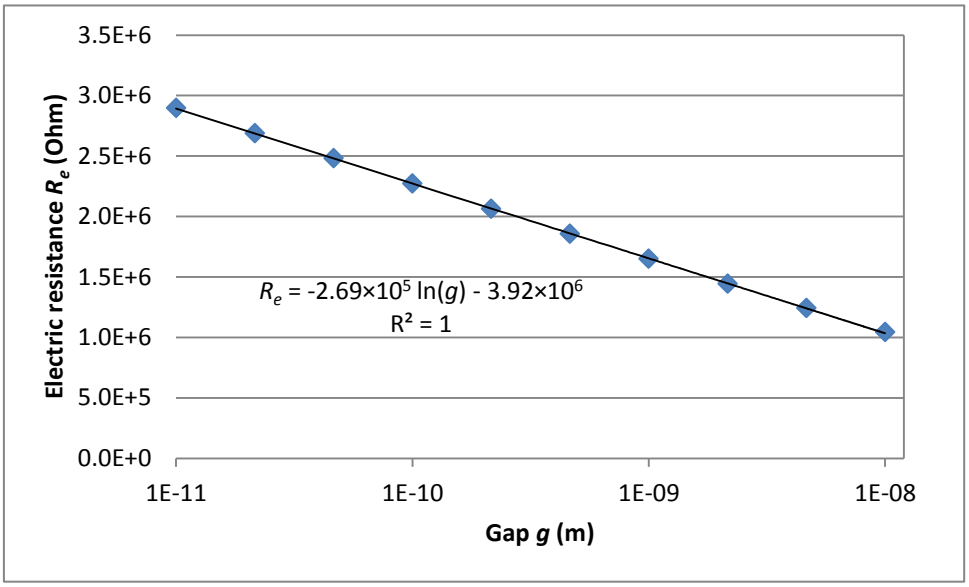

Figure S 8: Simulated electrical resistance vs. the gap distance and its fitting function. The errors of the simulation are within the rectangle boundaries.

The simulated electric resistance scaled with the logarithm of the gap distance as shown in Fig. S8. An analytic approximation was used to confirm this scaling law, very similar to the approach for the hydrodynamic resistance. All arguments were the same, except that the electrical resistance of a cuboid was (2):

$$R_{e\,cuboid} = \frac{\rho l}{wd}$$

Where ρ is the electrical resistivity of the medium.

$$R_e = \rho \int_{x_0}^{x_{end}} \frac{1}{wd} dx = \frac{6\eta}{\pi d_o \alpha} \left(\ln(x_{end}) - \ln(\frac{g}{\alpha}) \right) \propto -\ln(g)$$

As ln(x) does not vanish towards infinity, a meaningful upper limit x_{end} had to be chosen. An obvious choice was to stop the integration where the sector grew past the bead. The corresponding x coordinate in the sector could be found through geometrical relations:

$$x_{end,1} = \frac{d_b}{2} \tan\left[\frac{\alpha_1}{4} + \frac{\alpha_2}{2} \right]$$

The values found with this approximation differed less than 20% from the simulated results.

Summary

Both hydrodynamic- and electrical resistances were simulated with COMSOL for a bead which almost blocked the cantilever opening. An analytical approximation could confirm the observed scaling laws:

$$R_h \propto g^{-2}$$
$$R_e \propto -\ln(g)$$

Combining both relations and using the numerical solutions found through simulation these two resistances could be connected:

$$R_h = 2245.3 \times e^{\frac{2.006 \times (R_e + 3.92 \times 10^6)}{2.69 \times 10^5}}$$

Simulation and analytical approximation differed by ~20% when using the same material parameters. This difference is attributed to two factors: That A) the analytical approximations are based on simple geometries. And B) that the vector-field of the flow/current could only be correctly considered in the simulations. Errors due to numerical imprecisions in simulations and fitting were estimated below 1 percent.

Supporting citations

1. Siekman, H.E., and P.U. Thamsen. 2009. Strömungslehre für den Maschinenbau. 2nd ed. Springer, Berlin Heidelberg.

2. Tipler, P.A. 1999. Physics for scientists and engineers. 4th ed. W.H. Freeman and company, New York.